



An Emulsion Approach to Resolve the Paradox of 3D Printing of Very Soft Silicones

Clément Perrinet, Edwin-joffrey Courtial, Arthur Colly, Christophe Marquette, René Fulchiron

► To cite this version:

Clément Perrinet, Edwin-joffrey Courtial, Arthur Colly, Christophe Marquette, René Fulchiron. An Emulsion Approach to Resolve the Paradox of 3D Printing of Very Soft Silicones. *Advanced Materials Technologies*, 2020, pp.1901080. 10.1002/admt.201901080 . hal-02588371

HAL Id: hal-02588371

<https://hal.science/hal-02588371>

Submitted on 14 Dec 2022

HAL is a multi-disciplinary open access archive for the deposit and dissemination of scientific research documents, whether they are published or not. The documents may come from teaching and research institutions in France or abroad, or from public or private research centers.

L'archive ouverte pluridisciplinaire **HAL**, est destinée au dépôt et à la diffusion de documents scientifiques de niveau recherche, publiés ou non, émanant des établissements d'enseignement et de recherche français ou étrangers, des laboratoires publics ou privés.

Title:

An emulsion approach to resolve the paradox of 3D printing of very soft silicones

Authors name and affiliations:

Clément Perrinet¹, Edwin-Joffrey Courtial², Arthur Colly², Christophe Marquette², René Fulchiron^{1,}*

Mr. Clément Perrinet, Prof. René Fulchiron: Univ Lyon, Université Claude Bernard Lyon 1, CNRS, Ingénierie des Matériaux Polymères, UMR5223, F-69622, Villeurbanne, France

Corresponding Author: rene.fulchiron@univ-lyon1.fr

Dr. Edwin-Joffrey Courtial, Mr Arthur Colly, Dr Christophe Marquette 3d.FAB, Univ Lyon, Université Lyon1, CNRS, INSA, CPE-Lyon, ICBMS, UMR 5246, 43, Bd du 11 novembre 1918, 69622 Villeurbanne Cedex, France

Abstract

3D printing of silicone has been a challenge for medical applications for several years. The main property of medical silicone (mostly Polydimethylsiloxane) is its mechanical similitude with human tissues. The very soft tissues as prostate, skin, liver, etc, are of Young's modulus lower than 100 kPa. 3D printing for such soft materials is not as obvious as printing thermoplastic polymers. In this work, the goal was to elaborate formulations of Room-Temperature-Vulcanizing silicone leading to final materials of Young's modulus down to 25 kPa while being processable by Liquid Deposition Modeling, a layer by layer deposit of extruded filament. The main challenge is keeping the material with a sufficient firmness during the process to maintain the shape of the object but without increasing its final rigidity. Therefore, a RTV silicone was mixed with a hydrophilic liquid to create an emulsion of high yield stress behavior. Different emulsions were tested to optimize the composition on the basis of rheological measurements carried out to determine the yield stress variation and compare it to an emulsion model. Then, after printing and curing, the hydrophilic liquid is removed to create a material of fine porosity and consequently of low Young's modulus.

1. Introduction

Additive Manufacturing of Silicones for medical applications has been a challenge for several years.^[1-6] The main property of medical silicone (mostly Polydimethylsiloxane, PDMS) is its potential mechanical similitude with human tissues and its biocompatibility.^[7, 8] Young's modulus of all Human tissues is included in the range of 10 kPa to 10 MPa^[9, 10]. Above 1 MPa, it corresponds to cartilaginous tissues (trachea, esophagus, muscles...) ^[11-13] and under 100 kPa are very soft tissues ^[14-16] as prostate, skin, liver.... However, 3D printing of such soft PDMS to mimic those tissues is not as obvious as printing of classical polymers^[17] (PLA, ABS, photo resins...), mainly because of their very poor firmness in the liquid state. Moreover, for a prospective in vivo application, photo-sensible silicones are excluded since they are known as not compatible with living cell. Lastly, thermal variation of mechanical properties, as for Fused Deposition Modeling (FDM) system, is impossible because silicone is elastomeric and, without curing, it remains liquid at ambient temperature.

In a previous publication ^[18] we proposed a solution to print soft PDMS down to 2 MPa of Young's modulus. In the present work, a solution is proposed to print materials of Young's modulus down to 50 kPa. The selected additive manufacturing process is the simplest, known as Liquid Deposition Modeling (LDM), a derivative of the Fused Deposition Modeling (FDM) process which is basically an extrusion driven by a computer. In this process, the original PDMS formulation is made of two liquids which are mixed in suitable proportions. Then, the PDMS printing is conducted at the liquid state. It must be pointed out that a long enough pot-life is necessary to avoid a hasty hardening of the formulation. Then, once the shape is given to the formulation by extruding it through a die using a syringe, the cross-linking occurs to fix the shape. The main challenge here is to obtain a formulation liquid enough to be easily extruded but becoming rapidly hard enough to maintain the shape of the layer by layer made object. Nevertheless, this is generally fulfilled with PDMS formulations of high contents of silica and yield stress agents.^[18] The consequent drawback of these formulations is that, after curing, the rigidity becomes too high, making the 3D printing of PDMS a paradox. Therefore, a different strategy is needed to hope obtaining printable PDMS with very low Young's modulus after curing. As enounced in our previous work,^[18] the main rheological properties driving the printing

ability is the yield stress of the fluid material. The higher is the yield stress; the better is the quality of the printed object (even though it may induce very high values of extrusion pressure).

One of the most studied ways for enhancing the yield stress of the initial fluids consists in adding fillers in the formulation^[19-22] and tuning the interactions between particles to make them forming a network leading to a solid-like behavior at low strains. However, generally this also leads to raising the final rigidity of the material. As a result, increasing the yield stress of the initial silicone fluid becomes paradoxical with the aim of obtaining very soft printed pieces. Another way to generate a yield stress fluid is to make emulsions. In that regard, an important work on the rheological behaviors of concentrated emulsion has been conducted by Mason et al.^[23-25] Their conclusions were that the interfacial structure of the droplets, responsible of the droplets size and their chemical interactions with the continuous phase, governs the behavior.

This so-called “Mayonnaise effect” (leading to a yield stress fluid) in concentrated emulsions is well described in the literature^[23] as the formation of a continuous (percolated) network of inclusions in contact with one another at rest (no shear state). The network is called “jammed” under low shearing because of its elastic response in such conditions, meaning it will not break but rather will be deformed in a reversible way.^[26] Under stronger shearing, the network will break, and the system will flow as a liquid. The exact value of the shear stress separating both behaviors is called the yield stress and the emulsion is qualified as yield stress fluid (like the mayonnaise). To extend the metaphor, the mayonnaise has an elastic behavior under low stress gravity, meaning it keeps its shape, but will flow and will be easily spread with a knife, with a little more effort.^[27]

According to the literature the jammed state for stabilized emulsion is the state with a volume ratio of inclusions bigger than 0.645 leading to the droplet deformation without any external shearing. In this work, the emulsions are not stabilized and such a ratio cannot be reached because a phase inversion occurs underneath. However, even for lower values, the mayonnaise effect can be still effective. In that case, the yield stress is likely due to a percolation of the dispersed phase in the emulsion which produces certain elasticity for a volume ratio of inclusions much lower than the fraction of jamming. The percolation threshold is the first volume ratio where the contacts between droplets become numerous enough to form a

macroscopic continuous network. From this threshold, a non-zero yield stress appears. Nevertheless it can be very weak depending on the number and the strength of the interactions between droplets. From silicone oil-in-water emulsions, stabilized with sodium dodecyl sulfate (SDS), Mason et al.^[23, 25, 28] derived a semi-empirical relation between the yield stress, $\tau_{y,s}$ and the volume fraction of inclusions ϕ . For that purpose, they considered the plateau of storage modulus which appears in the low frequencies range for the percolated emulsions (G'_p) characteristic of a yield stress fluid behavior. It can be noticed that if this plateau modulus exists, its value is equivalent to $|G^*|$ because the loss modulus becomes much smaller than the storage modulus in that range. Moreover, from strain amplitude sweep measurements, they noticed the strain value from which the modulus starts to decrease ($\gamma_{y,s}$) indicating the limit of the linear viscoelastic domain due to the network destruction. Then, the yield stress was obtained from:

$$\tau_{y,s} = G'_p \gamma_y \quad (1)$$

Besides, by varying ϕ , they obtained a semi-empirical relation to describe G'_p :

$$G'_p \approx 1.7 \left(\frac{\sigma}{a} \right) \phi_{eff} (\phi_{eff} - \phi_c) \quad \text{for} \quad \phi_{eff} \geq \phi_c \quad (2)$$

where σ is the interfacial tension between oil and water, a is the droplet radius and ϕ_{eff} is the effective volume fraction of droplets which takes into account the presence of a water film around the droplets due to the surfactant SDS. Nevertheless, because the thickness of this film is dependent on ϕ ^[29], the expression of ϕ_{eff} is not trivial^[23, 25, 30]. However, in any case, it is of a few tens of nanometers thick so that from a droplet radius of a few hundreds of nanometers, ϕ_{eff} can be assimilated to ϕ . In Equation 2, the parameter ϕ_c is the critical volume fraction above which a yield stress threshold is observed. This parameter is generally considered by Mason et al.^[25] as the random close packing of monodisperse, undeformed spheres $\phi_c \approx 0.646$. Nevertheless, it has been reported as possibly much lower than this value, particularly in the case of attractive emulsions^[31-33] where a percolation between droplets can occur. From a quantitative point of view, as shown in Equation 2, the Laplace pressure scale σ/a is the important microscopic property which determines the level of plateau modulus.

Furthermore, the yield strain variation with the volume fraction^[23, 25] can be empirically expressed by :

$$\gamma_y \approx 0.3(\phi_{eff} - \phi_c) \quad (3)$$

Therefore, an empirical expression for the dependence of the yield stress on the volume fraction is obtained by multiplying Equation 2 and Equation 3:

$$\tau_{y,s}(\phi_{eff}) \approx 0.5 \left(\frac{\sigma}{a} \right) \phi_{eff} (\phi_{eff} - \phi_c)^2 \quad \phi_{eff} \geq \phi_c \quad (4)$$

This model shows the dependency of the yield stress on the interfacial tension and the size of particles. Practically, in order to obtain the highest possible yield stress, Equation 4 shows that the emulsion must be made of liquids with high interfacial tension, low droplet radius and, to the extent that the phase inversion is not attained, the largest concentration of the dispersed liquid is required.

In the present work, emulsions of two hydrophilic liquids in PDMS will be tested at different contents. The rheological behavior will be characterized to identify the best concentrations. Then, 3D printing experiments will be done and, after curing (and the removing of the hydrophilic liquid), the mechanical properties of the obtained material will be tested. **Figure 1** schematically shows the overall approach of this work.

More precisely, the hydrophilic liquids used to enhance the yield stress will be a polyethylene glycol of 400 g.mol⁻¹ of molecular weight (PEG 400) or the glycerol and make the printing possible. It can be mentioned that similar emulsions have already been tested in 3D printing by Rauzan et al.^[34] However, in their work, the dispersed phase was mainly constituted of water; PEG and sodium dodecyl sulfate being the surfactants used to stabilize the emulsion. The printing is then carried out with PDMS at the liquid state. Afterward, the PDMS continuous matrix is cross-linked while the shape is maintained owing to the yield stress of the emulsion. Lastly, the hydrophilic (sacrificial) part may be washed off by solvent extraction in order to leave a porous PDMS structure presenting a lowered Young's modulus.

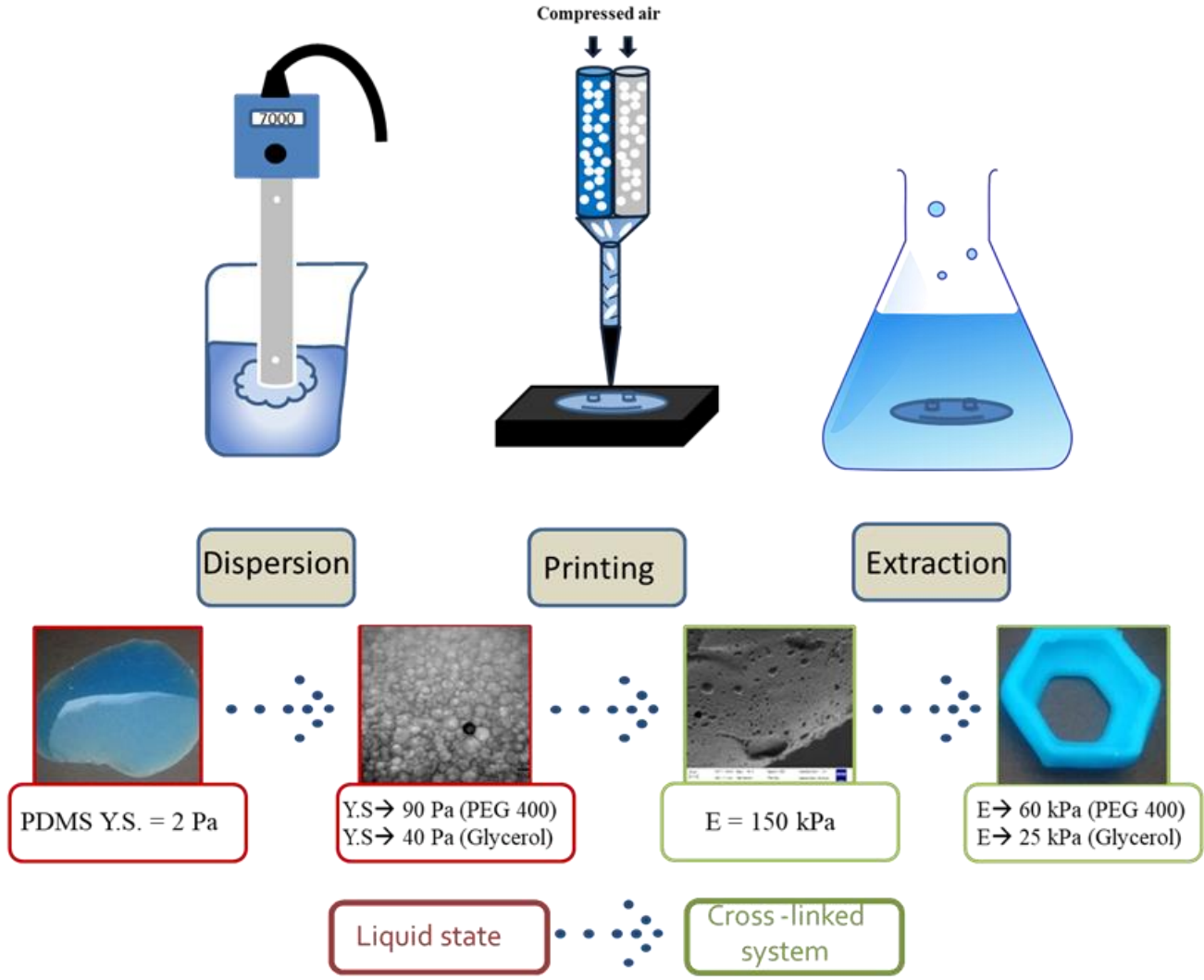


Figure 1: Evolution of the process, from liquid PDMS to solid soft PDMS. Y.S stands for Yield stress and E for Young modulus.

2-Results and discussions

2.1 Emulsions

2.1.1 Interfacial tension

First, optical observations were conducted to evaluate the interfacial tension^[35, 36]. As seen in **Figure 2**, the glycerol (or PEG 400) drop is sheared and gets an ellipsoidal shape. Then it relaxes to its original spherical shape. During the relaxation, the long (L) and the short (B) axes are measured.

From the time variation of B and L , the interfacial tension can be obtained using the deformability equation:^[36, 37]

$$D = D_0 \exp\left(\frac{-40(p+1)}{(2p+3)(19p+16)} \frac{\sigma}{\eta_m R_0} t\right) = D_0 \exp\left(-\frac{t}{\tau_0}\right) = \frac{L-B}{L+B} \quad (5)$$

where D_0 is the deformability parameter at the initial time t_0 , η_m the viscosity of the matrix (PDMS), p the viscosity ratio between the hydrophilic liquid and the PDMS, and R_0 the droplet radius before the shearing. In Equation 5, a relaxation time τ_0 is defined. This relaxation time is obtained from the fit of the deformability curve versus time.

Then σ is deduced from:

$$\sigma = \frac{(2p+3)(19p+16)}{40(p+1)} \frac{\eta_m R_0}{\tau_0} \quad (6)$$

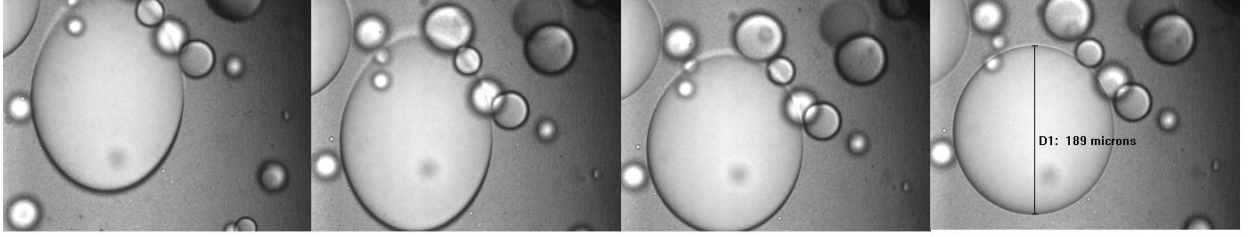


Figure 2: Relaxation of a glycerol droplet in liquid PDMS (Part B).

The viscosity values of the components necessary in Equation 6 were obtained from the complex viscosities measurements displayed in **Figure S1 in supporting information**. These measurements clearly show Newtonian behaviors for all the considered liquids. The obtained viscosity values are 1.52, 0.59 and 0.1 Pa.s for respectively PDMS, Glycerol and PEG 400. Hence, the viscosity ratios p are 0.38 for Glycerol and 0.066 for PG 400.

The interfacial tension values obtained from these measurements were of $7.3 \pm 0.6 \text{ mN.m}^{-1}$ for PEG 400/PDMS system and $25.6 \pm 1.4 \text{ mN.m}^{-1}$ for Glycerol/PDMS system.

2.1.2. Droplets size

Optical microscopic views were taken of both systems (PDMS/glycerol and PDMS/PEG 400) with an increasing volume ratio of hydrophilic content (see **Figure S2 in Supporting Information**). These images show an increasing of the droplet size with the volume ratio of hydrophilic liquid and an important polydispersity. In that regard, it can be mentioned that the mixing duration in Ultra-Turrax is a complex parameter to handle that cannot be extended a lot because, after 5 minutes of treatment, the self-heating becomes important modifying the viscosities and interfacial tension so that a longer exposition does not

significantly improve the size distribution. Moreover, in the case of Glycerol, the droplets appear generally larger than for PEG 400. From this type of pictures, the average size of the droplets was evaluated for each ratio in both PEG/PDMS and Glycerol/PDMS systems. It was impossible to claim to measure this mean droplet size with very high accuracy from those images and only rough values will be used in the following. Hence, according to the volume fractions, the average droplets measured radius varies from 1 to 7 μm for PEG 400 and from 1 to 17 μm for Glycerol (see **Table S3 in Supporting Information**). Moreover, from the pictures, it could be tempting to get information about the percolation threshold of the droplets network. However, due to high polydispersity and above all, the lack of resolution for low ratios, this is very tricky. Nevertheless, in any case, this threshold appears from volume fraction of dispersed phase much lower than 0.646 that is the expected value for a random close packing of monodisperse, undeformed spheres.

2.1.3. Yield Stress

(Top) shows the yield stress measurements of both PEG 400/PDMS and Glycerol/PDMS systems and their variations with the volume ratio of hydrophilic liquid. The variations of storage modulus with angular frequency are also shown in **Figure 3** (Bottom). The first obvious conclusion from these results is that the PEG 400 is much more efficient as thickening agent than the Glycerol in spite of its lower viscosity. This is clearly shown by the storage modulus curves where a plateau in the low frequency range is noticeable from much a lower volume fraction for PEG 400 than for glycerol. It must be admitted that results at even lower frequencies could have been interesting to clearly observe the presence of the plateau modulus and thus distinguish the percolation threshold. However, these measurements were not conclusive because of a lack of accuracy. Therefore, the values of yield stress ($\tau_{y,s}$) were taken at the maximum of stress growth curves (Top of **Figure 3**). It can be seen that a yield stress is observable in these stress/strain curves from volume fraction of PEG 400 or glycerol in accordance with the presence of the plateau modulus. Hence, the maximum of the yield stress appears for an amount of around 50% for the PEG 400 and 64% for the glycerol. Beyond these values, the yield stress and the storage modulus decrease remarkably indicating the phase inversion that leads to droplets of PDMS in the hydrophilic liquids (PEG 400 and Glycerol) of very low viscosities.

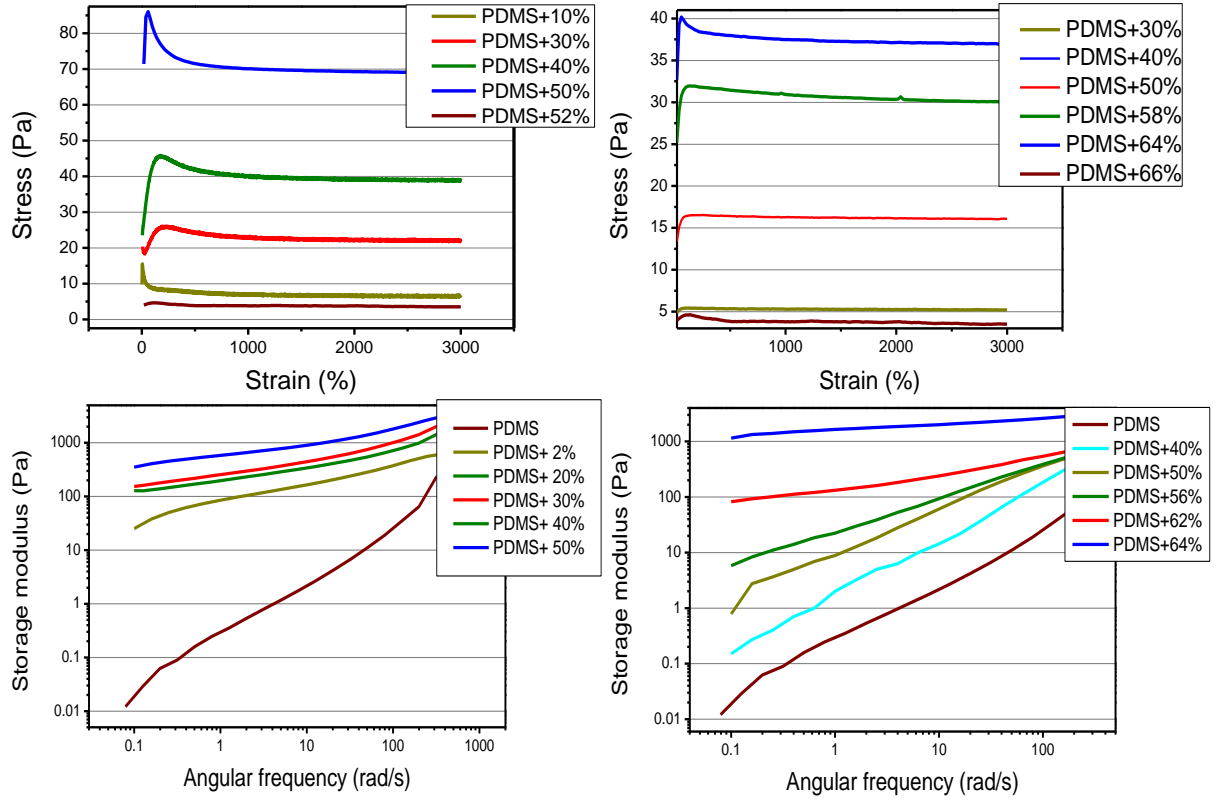


**Figure 3: Rheological characterization: Left Top: Yield stress measurements of PEG 400/PDMS (Part B) systems
Right Top: Yield stress measurements of Glycerol/PDMS (Part B) systems.
Left Bottom: Storage modulus versus angular frequency of PEG 400/PDMS (Part B) systems,
Right Bottom: Storage modulus versus angular frequency of Glycerol/PDMS (Part B) systems.**

Figure 4 shows the variation of the yield stress with the volume fractions of PEG 400 and Glycerol in PDMS. Again, despite its lower viscosity, the better efficiency of the PEG 400 to enhance the yield stress is clearly shown compared to the Glycerol. As an example, the yield stress is 8 times higher at a volume fraction of 0.5 using PEG 400. As already mentioned, the values of volume fraction at the percolation threshold (ϕ_c) could not be determined from the microscopic observations. Thus, the values of ϕ_c used to compare the Mason's model (Equation 4) with the experimental yield stress were adjusted and the fitting led to values of 0.2 and 0.21, respectively for PEG 400/PDMS and Glycerol/PDMS systems. These values can seem very low, especially in the case of PEG 400 recalling the value of 0.646 considered in the original model. However, these very low values are still in accordance with the storage modulus curves shown in **Figure 3** where, for example, a plateau modulus already appears from very low PEG 400 content. Such low value of percolation thresholds have been referenced in attractive emulsions^[33]. Yet, it must be recalled that the used PDMS contains around 4.5 vol% of silica. Thus, the possibility of a network formation including silica and PEG which has been reported for systems with higher silica amounts^[18] cannot be ruled out.

However, for high volume fractions of PEG, the emulsion formation is clear (see **Figure S2 in Supporting Information**) and its role in the yield stress level is evident. Moreover, the maximum volume fraction depends on the interfacial tension and the viscosity ratio. Exceeding this maximum value leads to the phase inversion and the loss of yield stress property of the fluid. **Figure 4** shows an important difference of maximum yield stress between PEG 400 and Glycerol. This may be explained by the difference of interfacial tension and viscosity ratio which impact the size of the inclusions. However, it can be recalled that the Ultra-Turrax mixing speed has been set constant for the present study but this parameter could also influence the dispersion state in the emulsion and, possibly, increase this maximum volume fraction. Hence, the further conclusion is that PEG 400 is more efficient to generate a yield stress, which is obviously beneficial for 3D printing. However, in order to finally obtain a softer material, increasing the maximum volume fraction before phase inversion may be researched for generating a higher porosity and hence, reducing the Young's modulus.

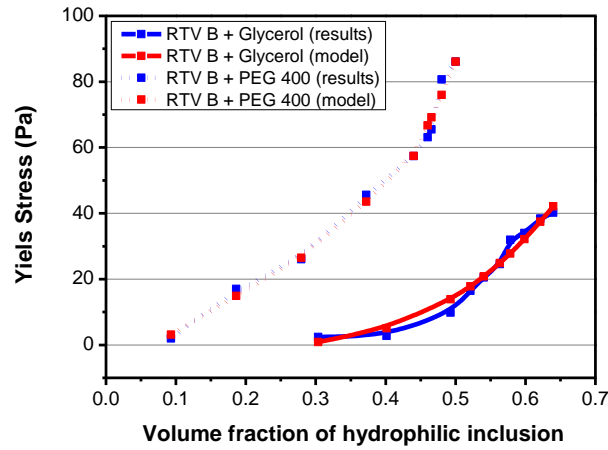


Figure 4: Yield Stress $\tau_{y,s}$ variation with volume fraction of PEG 400 and volume fraction of Glycerol in PDMS (Part B). Calculated curves (Model) are deduced from Equation 4 with an interfacial tension value of 7.3 mN.m^{-1} for PEG 400 and 25.6 mN.m^{-1} for Glycerol. The droplets radius a varies from 0.3 to $5 \text{ }\mu\text{m}$ for PEG 400 and from 3 to $35 \text{ }\mu\text{m}$ for Glycerol. From fitting, the obtained percolation threshold ϕ_c was 0.20 for PEG 400 and 0.21 for Glycerol

2.1.4 Printing

In the following 3D printing tests, the formulations with 64 vol% of glycerol (PDMS Gly64) and with 50 vol% of PEG 400 (PDMS PEG50) were chosen for their maximum yield stress of respectively 41 Pa and 90 Pa.

shows the 3D printing results obtained for the hexagonal object using the emulsions. This object was selected to challenge the material's properties. It is obvious that without preparing a silicone emulsion, the printing is totally inconceivable (n°2 in **Figure 5**). The yield stress of the PDMS 3503 is clearly too low (practically null); there is absolutely no holding of the object. On the contrary, by making an emulsion, an object of medium complexity can be printed with satisfactory fidelity. As discussed previously,^[18] the increase of the yield stress enables the printing of more complex structures. The first layers can be printed and withstand the weight of upper layers without collapsing.



Figure 5: Printing results, from left to right: 1: the control object, 2: the unmodified PDMS object after curing, 3: the PDMS+64vol% of glycerol object after curing and washing, 4: the PDMS +50vol% of PEG 400 after curing and washing.

Moreover, the yield stress difference between both emulsions leads to a variation in the printing quality. The PDMS PEG50 object, for which the yield stress of the initial formulation was 90 Pa is better shaped than the PDMS Gly64 object of which the emulsion yield stress was of 40 Pa.

2.2. Solvent Extraction and Mechanical Analysis

2.2.1. Solvent selection

The purpose of solvent extraction is to eliminate the hydrophilic liquid from the PDMS after curing to leave porosity and reduce Young's modulus of the cross-linked PDMS. The goal is then to remove all these liquid inclusions out of the PDMS matrix. Several solvents can be chosen, but hydrophilic solvents which can also swell PDMS at high temperatures are more appreciated because this should be helpful for the extraction by enhancing the access to the hydrophilic liquid. Ethanol and diethyl ether are well known hydrophilic solvents which swell PDMS.

The results for the best solvent selection are summarized in **Figure S4 in Supporting Information**. The tests were conducted on the PDMS PEG50 sample; the maximum mass loss expected (with the total

extraction of PEG 400) was of 52wt% (50 vol%). The swelling volume corresponds to the ratio between the volume of the sample swelled by the solvent and its initial volume^[38].

Results of the extraction are resumed here: water as only solvent does not swell cured PDMS and the mass loss measured was only of 40wt%. Diethyl ether swells the PDMS increasing its volume eight times and washing the totality of PEG 400 (52wt %) but this solvent obviously modify the PDMS getting harder. Water/ethanol 1:1 mixing swells lightly the PDS and wash 45wt% of the total mass. Finally boiling ethanol alone swells the PDMS and allows the washing of all PEG 400 without obviously altering the PDMS.

As shown by the result description, although the diethyl ether swells very well the PDMS and washes off the PEG 400, it alters the PDMS material, letting a deformed and shrunk sample with an apparent hardening. The explanation effect is out of the scope of this work but that makes the diethyl ether unacceptable. The water and the water/ethanol mix (50%-50% by weight) are less efficient in PDMS swelling and consequently, in washing PEG 400. Hence, the pure ethanol turned out to be the best solvent for this application.

2.2.2. TGA analyses

TGA analyses (degradation under helium atmosphere with a 5°C.min⁻¹ ramp to 600°C) were carried out to check the extraction of the hydrophilic component. **Figure 6** shows the superposition of curves that represent the raw PDMS, the raw hydrophilic liquid, the solid blend of both PDMS and hydrophilic liquid and the washed off sample after solvent swelling and drying. In both blends, it is shown that the hydrophilic liquid departure is from about 200°C. Then, the first PDMS degradation starts either at 400°C or 350°C depending on the ratio of polyols in the system^[39] since polyols make the PDMS burning at lower temperatures. Finally, in the range of 500- 600°C, the PDMS is degrading faster. The most important conclusion here is that the curves concerning the raw PDMS and the samples coming from the emulsions after washing are identical showing that after washing, all the hydrophilic liquid has been removed from the material without altering its thermal resistance.

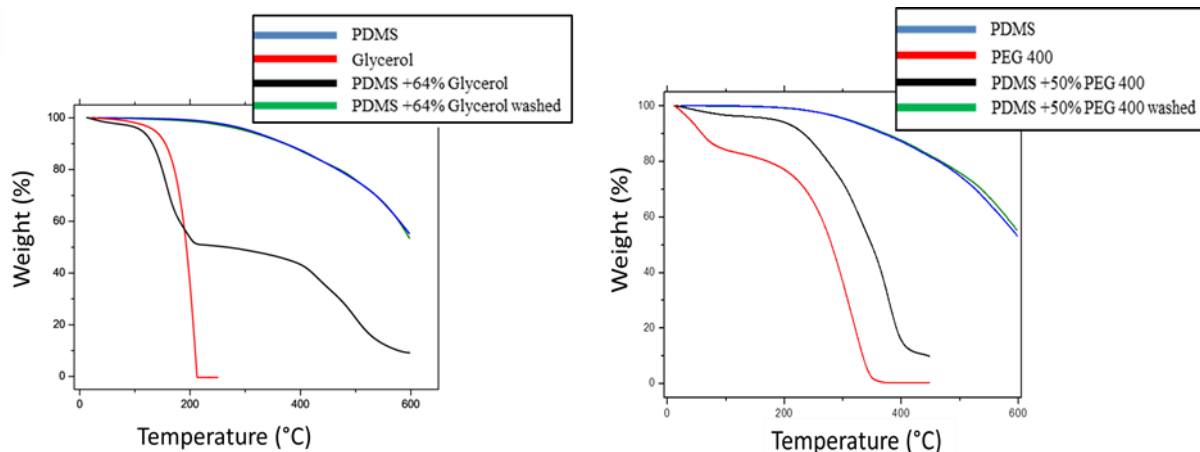


Figure 6: ATG analyses of PDMS Gly64 (top) and PDMS PEG50 (bottom) at different steps of the process and comparison with the raw hydrophilic liquid

2.2.3. SEM observations

SEM analyses allow the characterization of the porous matrix obtained after the extraction. In **Figure 7**, the pictures show the good extraction of the hydrophilic liquid, the pores size and the possible connections between pores. The heterogeneous distribution of the pores size is the same as before the cross-linking as it can be seen in **Figure S2 in Supporting Information**. For Glycerol/PDMS (right) formulation, the initial inclusions size and the high volume fraction of glycerol has led to the formation of macroscopic holes. Those holes were even visible during the preparation of the sample and could reach 0.3 mm. **The last image in Figure 7 shows the unwashed PDMS with 50 vol% of PEG 400 which is oozing out of the material as little droplets. This image is representative of all unwashed PDMS with PEG 400 or glycerol.**

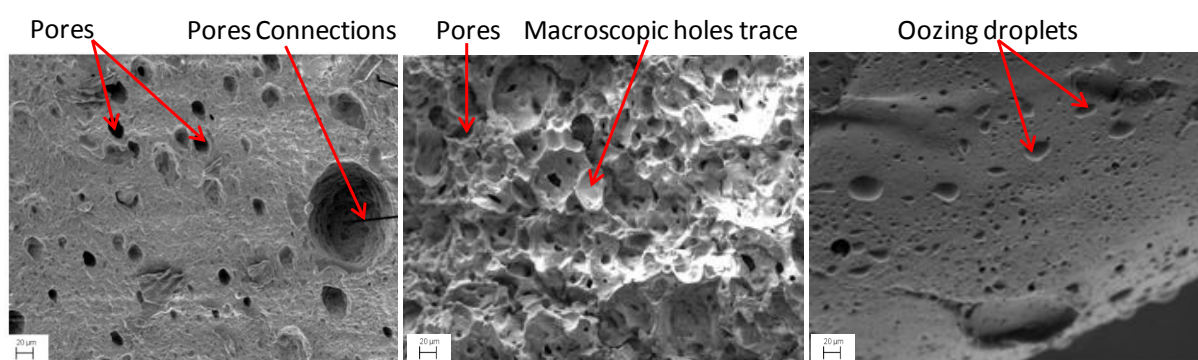


Figure 7: SEM pictures of PDMS PEG50 (left) and PDMS Gly64 (middle) after extraction, unwashed PDMS PEG50 (right). Scale bar is of 20 μ m.

2.2.4. Mechanical analyses

As previously explained, one of the main goals is to get a PDMS material with a very low Young's modulus to mimic this of soft human tissues under 100 kPa.^[14-16] The mechanical measurements shown in **Figure 8** witnesses a huge decreasing of Young's modulus (slopes of the curves) thanks to the proposed protocol. From 250 kPa of the initial PDMS Young's modulus, it is possible to go down to 60 kPa for the formulation with PEG 400 and even 25kPa for the system with glycerol. This last remarkable decrease of modulus by a factor of ten is obtained because of the high maximum fraction of glycerol which leads to a large porosity in the final material.

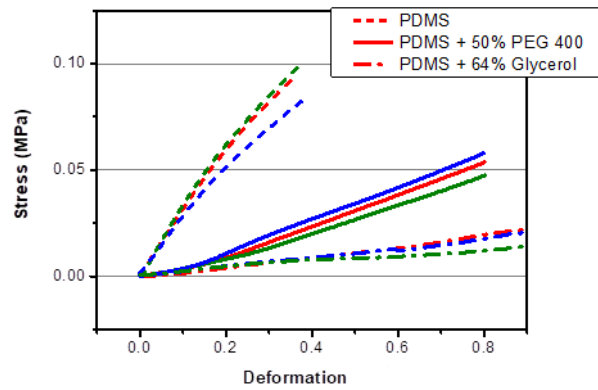


Figure 8: Compression measurements (repeated 3 times to show the good reproducibility) of unmodified PDMS silicone (dashed lines), PDMS modified with PEG 400 after extraction (solid lines), PDMS modified with Glycerol after extraction (dot-dashed lines)

3. Conclusion

The 3D printing of materials like PDMS is based on the ability to create a yield stress fluid from the initial uncured silicone. The value of this yield stresses impacts the panel of printable objects and the quality of the printing. Emulsions are few of the known yield stress fluids and the main idea of this work was to create an emulsion with uncured silica-poor PDMS and a viscous hydrophilic liquid to obtain a “mayonnaise like” system which is easily printable. As hydrophilic liquids, PEG 400 and glycerol have been chosen but the methods can be applied to other hydrophilic fluids. The panel of these other liquids should be extended as far as the interfacial tension is measurable and drives the energetic equilibrium of the system. Combined with the average inclusions size and the proportion of hydrophilic liquid, this physical value leads to the control of the yield stress which is well described by the Mason’s model. The innovation described in this work bears also on the ability to extract the hydrophilic liquid inclusions after the printing and the curing to

reach expected elastic behaviors by creating a porous system. Those elastic behaviors are directly linked to the liquid volume fraction introduced in the system. Such PDMS is then an efficient key to get one of the softer 3D printed PDMS.

4. Methods

- Emulsion: The BLUESIL® RTV 3503 silicone formulation from Elkem Silicones is a two parts liquid formulation made of Part A, containing vinyl groups and part B containing Si-H groups. Both parts have to be mixed in equal volume and the cross-linking by hydrosilylation results in a gel after approximately 20 min at ambient temperature (i.e. the pot life is of 20 min). It must be mentioned that this PDMS formulation contains 4.5 vol% of silica. The emulsion for 3D printing was prepared by mixing a volume of the sacrificial hydrophilic liquid with the desired volume of RTV of part A and part B. The hydrophilic liquid was either the PEG 400 (purity 98% from Sigma-Aldrich) or the glycerol (purity 96% from Sigma-Aldrich). PEG 400 and glycerol^[40] were chosen as sacrificial liquids because of their viscosity compatible with the manufacturing of an emulsion with uncured PDMS and their hydrophilic property. The emulsions were prepared using an Ultra-Turrax T50 Homogenizer (IKA) at 7000 tr.min^{-1} until the emulsion gets a gel consistency, if occurring, or for 5 min otherwise for lowest levels of hydrophilic liquids. Because of the relatively short pot life, a lot of measurements (rheology, interfacial tension...) could not be properly carried on the reactive blend of PDMS constituted of both components A and B. Thus these experiments were performed with emulsions of hydrophilic liquid in only one component of the PDMS, namely Part B. Nevertheless it must be mentioned, firstly, that the viscosities of Part A and Part B are very close and, secondly, that some tests, not presented in the following, have been carried out using Part A and the conclusions were very similar.

- Interfacial tension measurement: According to the work of Utracki^[35, 36] and previous tests in our lab,^[37] the measurements of the interfacial tension between silicone and PEG400 or glycerol were carried out, using a Leica DM2700 M microscope (transmission) with 20× lens coupled with a shearing stage Linkam CSS-450. Strain relaxation experiments were conducted by applying an oscillatory strain of 70% at 5Hz, for 10 s

to deform the studied droplet of hydrophilic liquid imbedded in PDMS. Then pictures were taken at 40 images per second, allowing us to follow the droplet retraction.

- Rheological tests: The rheological measurements were conducted at ambient temperature using an ARES G2 rheometer (TA Instruments, USA) with a cone-plate geometry of 25 mm of diameter and a cone angle of 0.1002 rad. The yield stress measurements were made in transient mode carrying out a stress growth experiment at a constant strain rate of 1 s^{-1} . The stress/strain curve presented a maximum of stress which was taken as the static yield stress value. The viscosity measurements of each liquid (PDMS, PEG400 and glycerol), necessary for the interfacial tension evaluations, were conducted using a Couette system with a 27 mm cup diameter and a 2.34 mm gap between walls of concentric cylinders. After a soak time of 300 s, a frequency sweep was conducted from 1 to 100 rad.s^{-1} at a strain of 1%.

- 3D Printing process: A Liquid Deposition Modeling (LDM) device with a COSMED 333 Cartesian 3D printer (Tobeca®, France) of 10 μm movement precision was used to print the emulsions. Bi-component cartridges of 50 mL (Nordson EFD, USA) were filled with the PDMS inks. These cartridges were fitted with a static mixer positioned upstream of a 200 μm diameter conical nozzle (Nordson EFD, USA). The extrusion was ensured using a pneumatic system, Equalizer and Ultimus V (Nordson EFD, USA). The dispensing pressure was adapted for each emulsion. The 3D printing was controlled with the Repetier Host software (Repetier, V2.0.1, Germany) at a printing speed of 10 mm.s^{-1} . The STL file was this of a homemade hexagonal model of medium complexity ^[18]. It is non-print travel-free, a small overhang of 5° (0 being the vertical). The file was sliced with the Slic3r software (Slic3r, V3, Italia) using adapted printing parameters. The control sample was printed with Verowhite resin using the Object30 Pro 3D printer (Stratasys, USA).

- Solvent extraction: The cross-linked silicone containing the hydrophilic liquid was immersed in a boiling selected solvent for 12 h and dried at 80°C for 12 h and at 100°C for another 12 h. The sample is a cylinder of 13 mm of diameter and 7 mm width, designed for mechanical characterization.

- Purification measurements: The first analysis was conducted by measuring the mass lost after extraction. TGA tests were conducted using a Q500 TGA (TA Instruments), with a temperature ramp of 5°C.min⁻¹ up to 600°C.
- Optical microscopic observations of the uncured emulsions to evaluate the droplets sizes were made using an Olympus BX 41 microscope in transmission mode. The droplet sizes distributions were obtained from typical parts images by measuring the size of 50 droplets. For the cured systems, a Merlin Zeiss SEM was used to characterize their porosity. A 1 kV electron beam was used in high vacuum with a zoom ×200.
- Mechanical Characterization: Compression tests were carried out to determine Young's modulus. A sample of 13 mm of diameter and 7 mm width was compressed within 25 mm plates on an ARES G2 at 0.01 mm.s⁻¹ for 600 s. From the force measurement, the nominal stress was obtained by dividing the measured force by the sample section (132.7 mm²). The nominal strain was obtained by dividing the plate displacement by the initial sample thickness. Then, Young's modulus was obtained from the slope of the stress/strain plot for the first 20 % of strain.

Supporting Information

Supporting Information is available from the Wiley Online Library

Acknowledgments:

This work was supported by the French government through FASSIL project, selected by FUI (Fonds Unique Interministériel) and by the “region Auvergne-Rhône-Alpes”. Special thanks to Jean-Marc Francès and Damien Djian from Elkem Silicones for materials supply and very helpful discussions. The authors also acknowledge the “Centre Technologique des Microstructures (CTμ)” of University Lyon 1 for the SEM experiments and especially Pierre Alcouffe of IMP, UMR5223 laboratory.

Conflict of Interest:

The authors declare no conflict of interest.

Keywords:

Additive Manufacturing, Silicone, Yield Stress Fluid, Emulsion, Soft Materials.

- [1] B. Berman, *Business Horizons* **2012**, 55, 155.
- [2] K. S. Boparai, R. Singh, *Reference Module in Materials Science and Materials Engineering*, Elsevier **2017**
- [3] D. Bourell, J. P. Kruth, M. Leu, G. Levy, D. Rosen, A. M. Beese, A. Clare, *CIRP Annals* **2017**, 66, 659.
- [4] J.-Y. Lee, J. An, C. K. Chua, *Appl. Mater. Today* **2017**, 7, 120.
- [5] P. Parandoush, D. Lin, *Compos. Struct.* **2017**, 182, 36.
- [6] E.-J. Courtial, *PhD Thesis*, Université Claude Bernard Lyon 1, France, **2015**.
- [7] J. Giannatsis, V. Dedoussis, *Int. J. Adv. Manuf. Tech.* **2009**, 40, 116.
- [8] M. Gajewski, R. Szczerba, S. Jemioło, *Procedia Eng.* **2015**, 111, 220.
- [9] M. Z. Ansari, S. K. Lee, C. D. Cho, *Key Eng. Mater.* **2007**, 1241, 345
- [10] H. Seitz, C. Tille, S. Irsen, G. Bermes, R. Sader, H.-F. Zeilhofer, *Int. Congr. Ser.* **2004**, 1268, 567.
- [11] M. Malvè, A. Pérez del Palomar, O. Trabelsi, J. L. López-Villalobos, A. Ginel, M. Doblaré, *Int. Commun. Heat. Mass* **2011**, 38, 10.
- [12] J. K. Rains, J.L. Bert, C.R. Roberts, P.D. Paré, *J. Appl. Physiol.* **1992**, 219, 25.
- [13] O. Trabelsi, A. P. del Palomar, J. L. López-villalobos, A. Ginel, M. Doblaré, *Med. Eng. Phys.* **2010**, 32, 76.
- [14] T. A. Krouskop, T. M. Wheeler, F. Kallel, B. S. Garra, T. Hall, *Ultrason. Imaging* **1998**, 20, 260.
- [15] P. Li, S. Jiang, Y. Yu, J. Yang, Z. Yang, *J. Mech. Behav. Biomed.* **2015**, 49, 220.
- [16] M. Zhang, P. Nigwekar, B. Castaneda, K. Hoyt, J. V. Joseph, A. di Sant'Agnese, E. M. Messing, J. G. Strang, D. J. Rubens, K. J. Parker, *Ultrasound Med. Biol.* **2008**, 34, 1033.
- [17] F. Liravi, E. Toyserkani, *Addit. Manuf.* **2018**, 24, 232
- [18] E.-J. Courtial, C. Perrinet, A. Colly, D. Mariot, J.-M. Frances, R. Fulchiron, C. Marquette, *Addit. Manuf.* **2019**, 28, 50.
- [19] M. I. Aranguren, E. Mora, J. V. D. Jr., C. W. Macosko, *J. Rheol.* **1992**, 36, 1165.
- [20] M. M. Rueda, M.-C. Auscher, R. Fulchiron, T. Périé, G. Martin, P. Sonntag, P. Cassagnau, *Prog. Polym. Sci.* **2017**, 66, 22.
- [21] A. Fall, F. Bertrand, G. Ovarlez, D. Bonn, *Phys. Rev. Lett.* **2009**, 103, 178301.
- [22] S. Asakura, F. Oosawa, *J. Poly. Sci.* **1958**, 33, 183.
- [23] H. S. Kim, T. G. Mason, *Adv. Colloid Interface Sci.* **2017**, 247, 397.
- [24] H. S. Kim, F. Scheffold, T. G. Mason, *Rheol. Acta* **2016**, 55, 683.
- [25] T. G. Mason, J. Bibette, D. A. Weitz, *J. Colloid Interface Sci.* **1996**, 179, 439.
- [26] P. Coussot, *Rheophysics - Matter in All Its States*, Springer **2014**, Chap 6, 201.
- [27] H. A. Barnes, *Colloid Surf. A.* **1994**, 91, 89.
- [28] T. G. Mason, F. Scheffold, *Soft Matter* **2014**, 10, 7109.
- [29] F. Leal-Calderon, V. Schmitt, J. Bibette, *Emulsion science: basic principles*, Springer Science & Business Media, **2007**.
- [30] J. N. Wilking, T. G. Mason, *Phys. Rev. E* **2007**, 75, 041407.
- [31] S. S. Datta, D. D. Gerrard, T. S. Rhodes, T. G. Mason, D. A. Weitz, *Phys. Rev. E* **2011**, 84, 041404.
- [32] J. Bibette, T. G. Mason, H. Gang, D. A. Weitz, P. Poulin, *Langmuir* **1993**, 9, 3352.
- [33] T. B. J. Blijdenstein, E. van der Linden, T. van Vliet, G. A. van Aken, *Langmuir* **2004**, 20, 11321.
- [34] B. M. Rauzan, A. Z. Nelson, S. E. Lehman, R. H. Ewoldt, R. G. Nuzzo, *Adv. Funct. Mater.* **2018**, 28, 1707032.
- [35] A. Luciani, M. F. Champagne, L. A. Utracki, *J. Polym. Sci., Part B: Polym. Phys.* **1997**, 35, 1393.
- [36] L. A. Utracki, *J. Rheol.* **1991**, 35, 1615.
- [37] Y. Deyrail, R. Fulchiron, P. Cassagnau, *Polymer* **2002**, 43, 3311.
- [38] C. V. Rumens, M. A. Ziai, K. E. Belsey, J. C. Batchelor, S. J. Holder, *J. Mater. Chem. C* **2015**, 3, 10091.
- [39] J. D. Jovanovic, M. N. Govedarica, P. R. Dvornic, I. G. Popovic, *Polym. Degrad. Stab.* **1998**, 61, 87.
- [40] P. Mazurek, S. Hvilsted, A. L. Skov, *Polymer* **2016**, 87, 1.